Universitat de Barcelona

Institut de Ciències del Cosmos

IEEC

Evidence of coupling between the thermal and nonthermal emission in the gamma-ray binary LS I +61 303 through optical observations

X. Paredes-Fortuny, M. Ribó, V. Bosch-Ramon, J. Casares, O. Fors, J. Núñez, and D. del Ser Badia

Variable Galactic Gamma-ray Sources
5 May 2015, Heidelberg

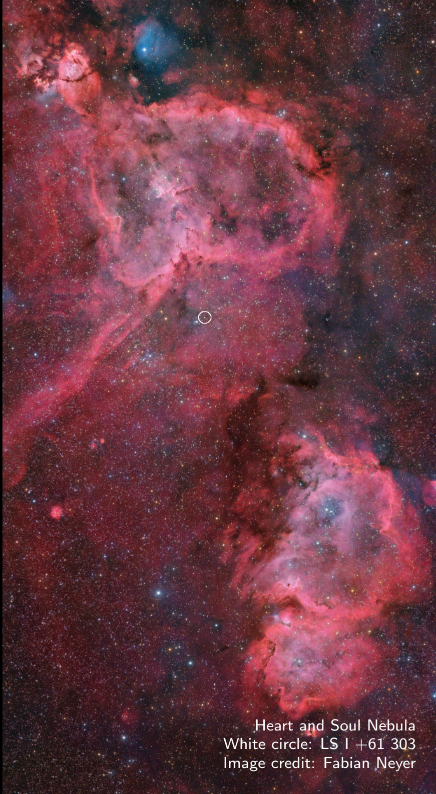

Outline

Outline

γ-ray binaries with Be star I

What are Be/γ-ray binaries?

Be/γ-ray binaries where the companion is a **Be** star. There are **three Be/γ-ray binaries currently known**, namely **LS I +61 303**, PSR B1259$-$63 and HESS J0632+57 (Albert et al. 2006, Hinton et al. 2009, Aharonian et al. 2005, Casares et al. 2012).

What are Be stars?

Are non-supergiant **fast-rotating early type stars** which at some time have shown emission lines (e.g. Negueruela 1998).

γ-ray binaries with Be star II

Nonthermal photons from gamma-ray binaries: **shocks+synchroton+IC**

Thermal photons from gamma-ray binaries: **star+disk**

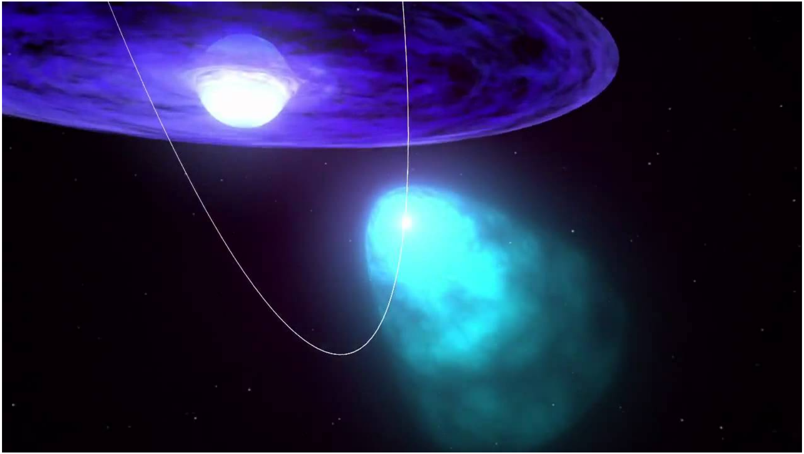

Figure 1 : Sketch of the scenario of the gamma-ray binary PSR B1259−63. From NASA.

γ-ray binaries with Be star II

Nonthermal photons from gamma-ray binaries: **shocks+synchroton+IC**

Thermal photons from gamma-ray binaries: **star+disk**

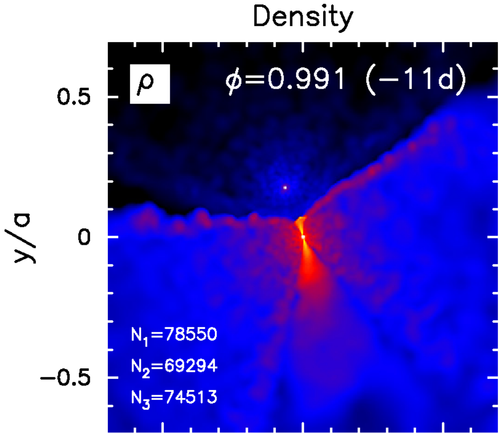

Figure 1 : Density map from **SPH simulation** of PSR B1259-63, **11 days prior to periastron**. From Takata et al. (2012), see also Okazaki et al. (2011).

Description of LS I +61 303 I

LS I +61 303

Is a γ-ray binary composed by an optical **Be** (B0 Ve) star ($V \sim 10.8$) and a **compact companion** orbiting in a highly eccentric orbit with a **period of 26.496 d** (Gregory 2002).

- **Modulated emission** has been detected in radio, optical photometry, Hα spectroscopy, X-rays, GeV, and TeV (see Moldón 2012 and references therein).
- Frail and Hjellming (1991) obtained a **distance** of $\sim 2.0 \pm 0.2$ kpc.
- Paredes & Figueras (1986) detected **optical variability** and Mendelson & Mazeh (1989) suggested a 26.5 d optical periodicity.
- Aragona et al. 2009 found an **orbital solution** that supports $e = 0.54 \pm 0.03$. Resulting in $d_{\mathrm{apa}}/d_{\mathrm{peri}} \sim 3$, with $d_{\mathrm{apa}} = 0.64$ and $d_{\mathrm{peri}} = 0.19$

Description of LS I +61 303 II

- LS I +61 303 shows a **∼ 4.6 yr superorbital modulation** in **Radio flux and phase of the maximum** (Fig.-left; from Gregory 2002) and **$EW_{H\alpha}$ flux** (Fig.-right; from Zamanov et. al 2013).

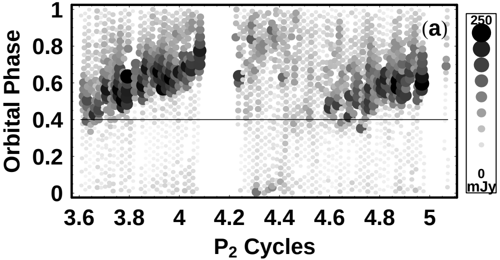

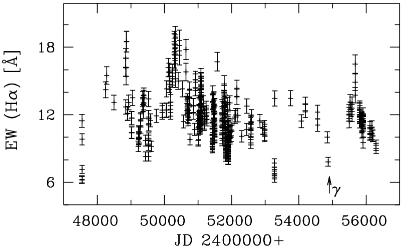

- This suggests that the superorbital variability is related to periodic **changes in the mass-loss rate** of the Be star and/or **variations in the circumstellar disk**.

- The superorbital variability in the **microquasar** scenario has also been explained using a precessing jet (see Massi & Torricelli-Ciamponi 2014 and references therein).

Description of LS I +61 303 III

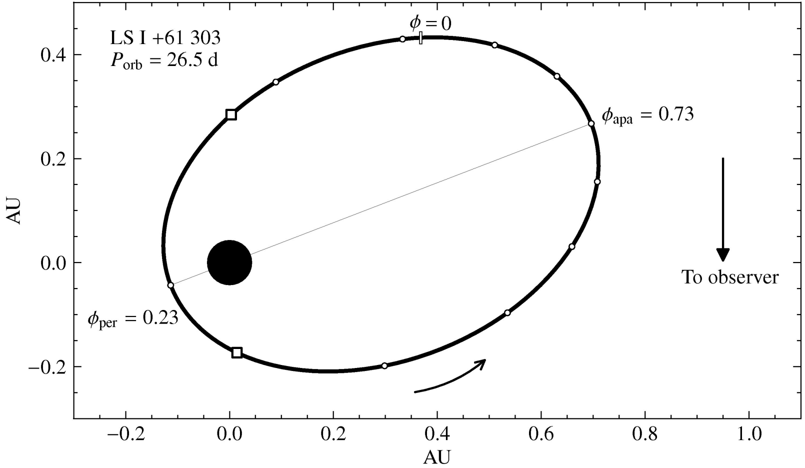

Figure 2 : Orbit of the **compact object (black ellipse)** around the massive star **LS I +61 303 (black filled circle)**. Small circles are plotted every 0.1 orbital phases. From Moldón (2012).

Description of LS I +61 303 III

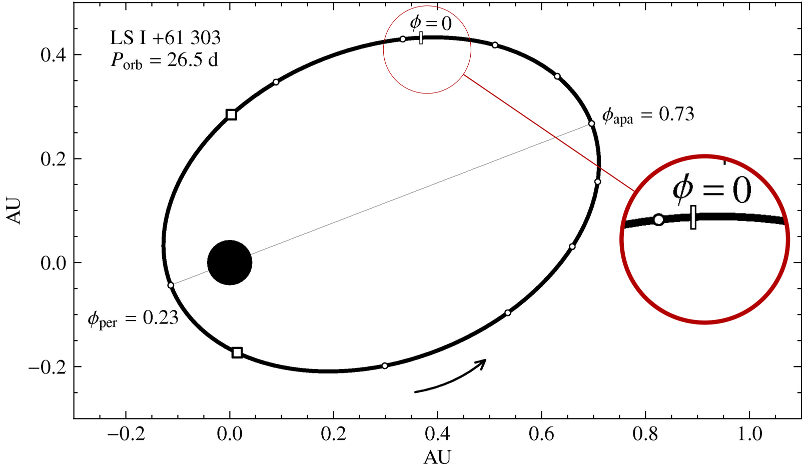

Figure 2 : Orbit of the **compact object (black ellipse)** around the massive star **LS I +61 303 (black filled circle)**. Small circles are plotted every 0.1 orbital phases. From Moldón (2012).

Description of LS I +61 303 III

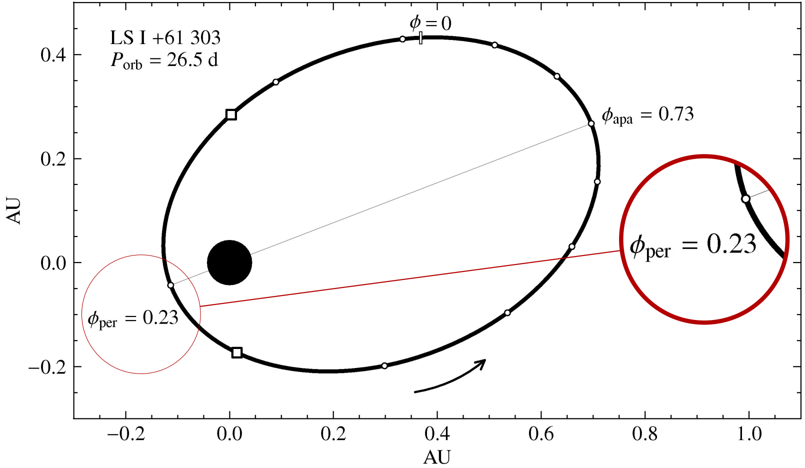

Figure 2 : Orbit of the **compact object (black ellipse)** around the massive star **LS I +61 303 (black filled circle)**. Small circles are plotted every 0.1 orbital phases. From Moldón (2012).

Description of LS I $+61$ 303 III

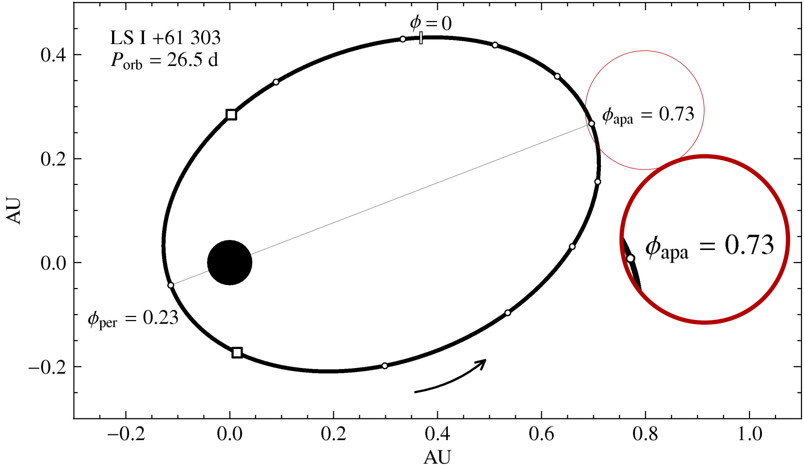

Figure 2 : Orbit of the **compact object (black ellipse)** around the massive star **LS I $+61$ 303 (black filled circle)**. Small circles are plotted every 0.1 orbital phases. From Moldón (2012).

Outline

Observations with TFRM I

Telescope Fabra ROA Montsec (TFRM)

The optical photometric observations of this project are currently made with the **robotic** telescope TFRM, installed at the *Observatori Astronòmic del Montsec* (Lleida, Spain) (Fors et al. 2013)[1].

- Corrector plate of **0.5 m aperture** and 0.78 m primary mirror.
- Refurbished Baker-Nunn Camera.
- Focal ratio f/0.96.
- **$4.4^\circ \times 4.4^\circ$ field of view** with a pixel scale of $3.9''$/pixel.
- **Passband filter $\lambda > 475$ nm**. The QE of the CCD is 60% at 550 nm.

[1] We want to thank all the TFRM team for preparing and carrying out the optical observations.

Observations with TFRM II

- We report data between **July 2012** and **March 2015** **(2.6 yr), in 19 different orbital cycles**.
- The **exposure time** ranges from **5.0 to 8.0 s** ($V \sim 10.8$).
- LS I +61 303 has been **observed** around **20 times per night**.
- **Observed** in good atmospheric conditions for a total of **101 nights** ($\sim$ 2400 science images + calibration images!).
- We have used **10 reference stars** (optical photometric calibration), obtaining a photometric **precision of $\sim$ 7 mmag** at 1 σ confidence level.

Reduction and analysis I

- We have developed a **pipeline written in Python** to reduce and analyze the data through **differential photometry**.
- The main steps are: **image calibration**, **quality control**, **astrometric reduction** and **photometric extraction** for all the stars in the image.

Reduction and analysis II

- We have used the following **algorithm** to **correct the lightcurves**:

  1. For each image (i) and star (j), we compute its magnitude difference with respect to the first image: $\Delta m_{\mathrm{i,j}} = m_{\mathrm{i,j}} - m_{1,\mathrm{j}}$
  2. We perform a weighted ($w_{\mathrm{j}} = 1/\sigma_{\mathrm{j}}^2$) average of $\Delta m_{\mathrm{i,j}}$ using all the stars, obtaining: $\Delta\overline{m}_{\mathrm{i}}$ (image correction)
  3. We correct the non-corrected photometry for each image (i) using $\Delta\overline{m}_{\mathrm{i}}$
  4. We compute the new σ_{j} using the corrected photometry
  5. We select the 10 reference stars with lowest σ (at angular distance $< 0.4^\circ$ with respect to LS I +61 303). We iterate until the selected stars do not change
  6. We assign to the mean magnitude the value of 10.7

- We compute **nightly averages** with the photometry of individual images for each night. The **uncertainty** is obtained with the standard deviation of the photometry of the individual images for each night.

Outline

Data from Liverpool Telescope

Liverpool Telescope

We also considered **contemporaneous $\mathbf{EW_{H\alpha}}$ data** obtained using the FRODOspec spectrograph on the robotic 2.0 m Liverpool telescope at the *Observatorio del Roque de Los Muchachos* (La Palma, Spain).

- LS I +61 303 has been **observed** with **one 600 s exposure per night**.
- The data span from **July 2012** to **December 2014** **(2.4 yr), in 17 different orbital cycles**.
- **Observed** in good atmospheric conditions for a total of **136 nights**.
- The $EW_{\mathrm{H}\alpha}$ precision is of **$\sim$1 Å** (individual $EW_{\mathrm{H}\alpha}$ uncertainties are assumed at 10% level).
- The data have been obatained and reduced as in Casares et al. (2012)

Outline

Results I

Results of the *Optical photometry* and *$EW_{\mathrm{H}\alpha}$ spectroscopy*:

- LS I +61 303 has been **observed in 3 different observational campaigns** centered at autumn of 2012, 2013 and 2014. Hereafter **Seasons 1, 2 and 3**, respectively.
- Results on **Seasons 1 and 2** have already been **published** in **Paredes-Fortuny et al. (2015)**.
- Results on **Season 3** are presented here for the **first time**.

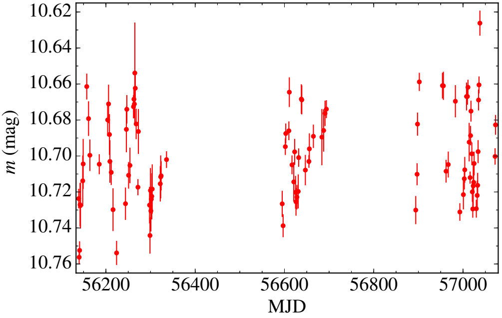

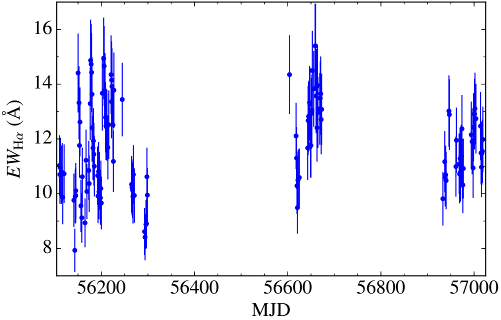

Results I

Results of the *Optical photometry* and *$EW_{\mathrm{H}\alpha}$ spectroscopy*:

- LS I +61 303 has been **observed in 3 different observational campaigns** centered at autumn of 2012, 2013 and 2014. Hereafter **Seasons 1, 2 and 3**, respectively.
- Results on **Seasons 1 and 2** have already been **published** in **Paredes-Fortuny et al. (2015)**.
- Results on **Season 3** are presented here for the **first time**.

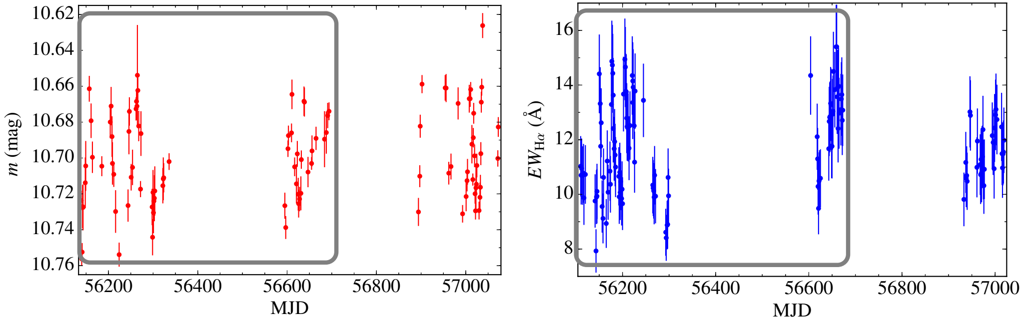

Results I

Results of the *Optical photometry* and *$EW_{\mathrm{H}\alpha}$ spectroscopy*:

- LS I +61 303 has been **observed in 3 different observational campaigns** centered at autumn of 2012, 2013 and 2014. Hereafter **Seasons 1, 2 and 3**, respectively.
- Results on **Seasons 1 and 2** have already been **published** in **Paredes-Fortuny et al. (2015)**.
- Results on **Season 3** are presented here for the **first time**.

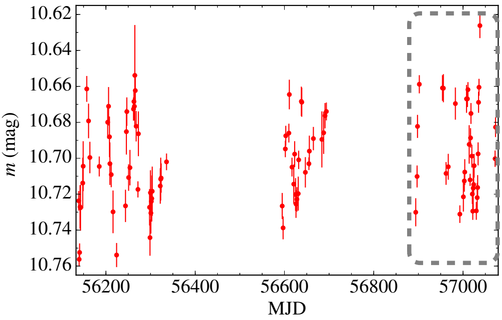

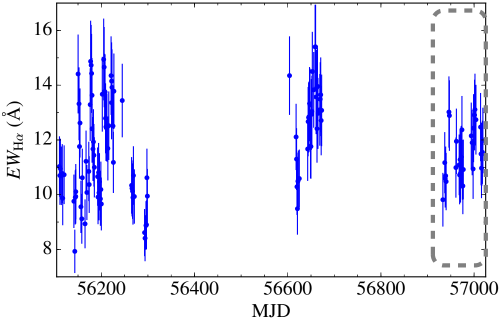

Results II

- The *photometry* shows a **broad maximum just after apastron**.
- The $EW_{\mathrm{H}\alpha}$ *spectrocopy* shows a **broad maximum just before apastron**.
- The lightcurves exhibit a **large scatter.**

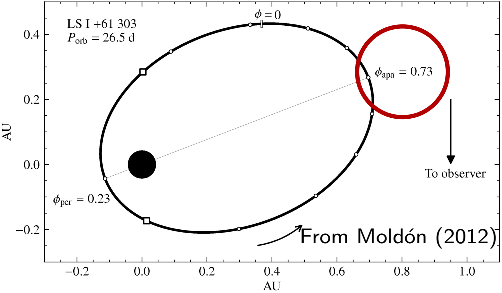

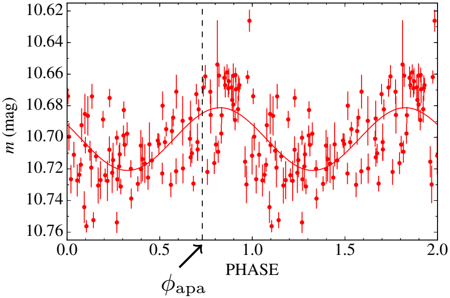

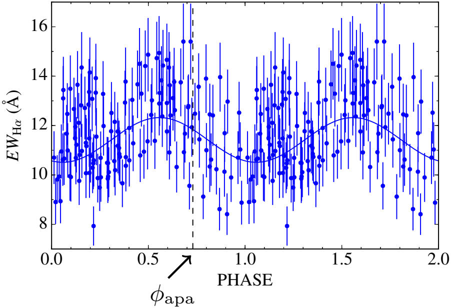

Results III

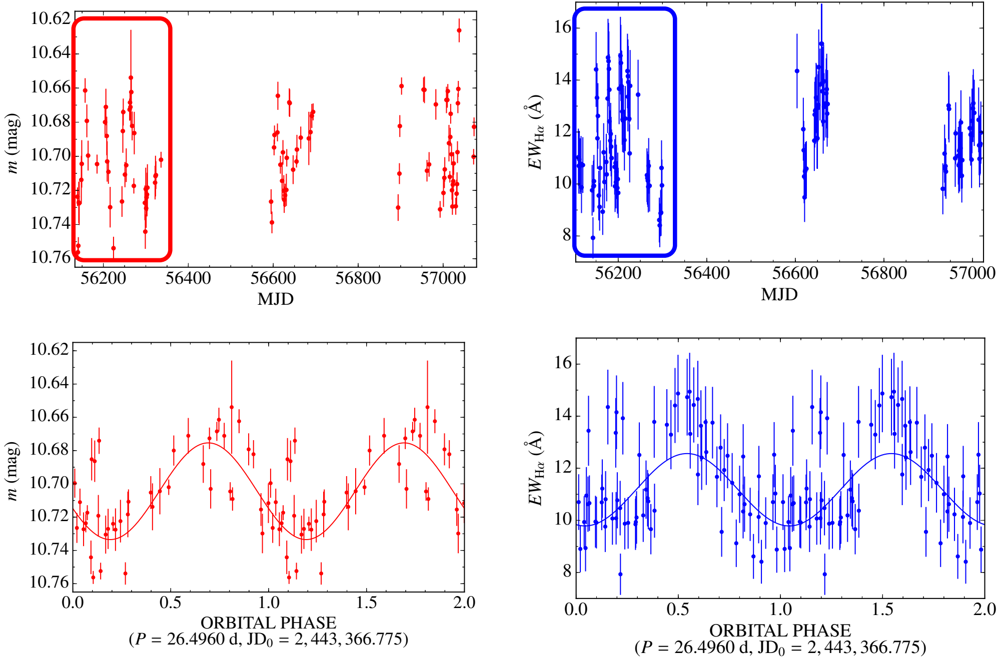

10.62
10.64
10.66
10.68
10.70
10.72
10.74
10.76
m (mag)
56200
56400
56600
56800
57000
MJD
16
14
12
10
8
$EW_{H\alpha}$ (Å)
0.0
0.5
1.0
1.5
2.0
ORBITAL PHASE
(P = 26.4960 d, JD_0 = 2, 443, 366.775)

Results III

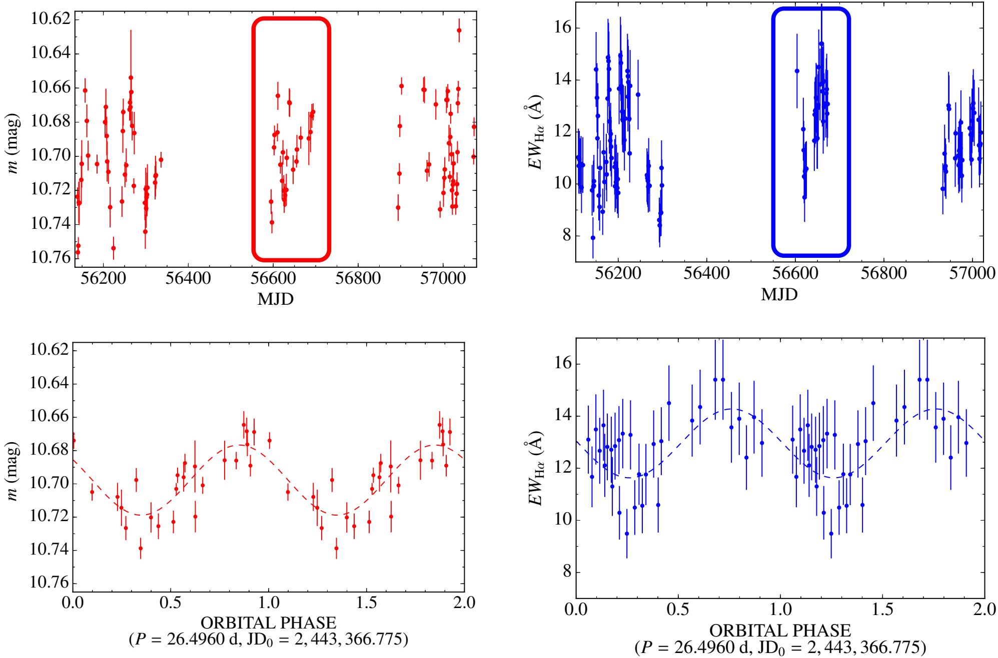

10.62
10.64
10.66
10.68
10.70
10.72
10.74
10.76
m (mag)
56200
56400
56600
56800
57000
MJD
16
14
12
10
8
$EW_{\mathrm{H}\alpha}$ (Å)
56200
56400
56600
56800
57000
MJD
10.62
10.64
10.66
10.68
10.70
10.72
10.74
10.76
m (mag)
0.0
0.5
1.0
1.5
2.0
ORBITAL PHASE
(P = 26.4960 d, JD_0 = 2, 443, 366.775)
16
14
12
10
8
$EW_{\mathrm{H}\alpha}$ (Å)
0.0
0.5
1.0
1.5
2.0
ORBITAL PHASE
(P = 26.4960 d, JD_0 = 2, 443, 366.775)

Results III

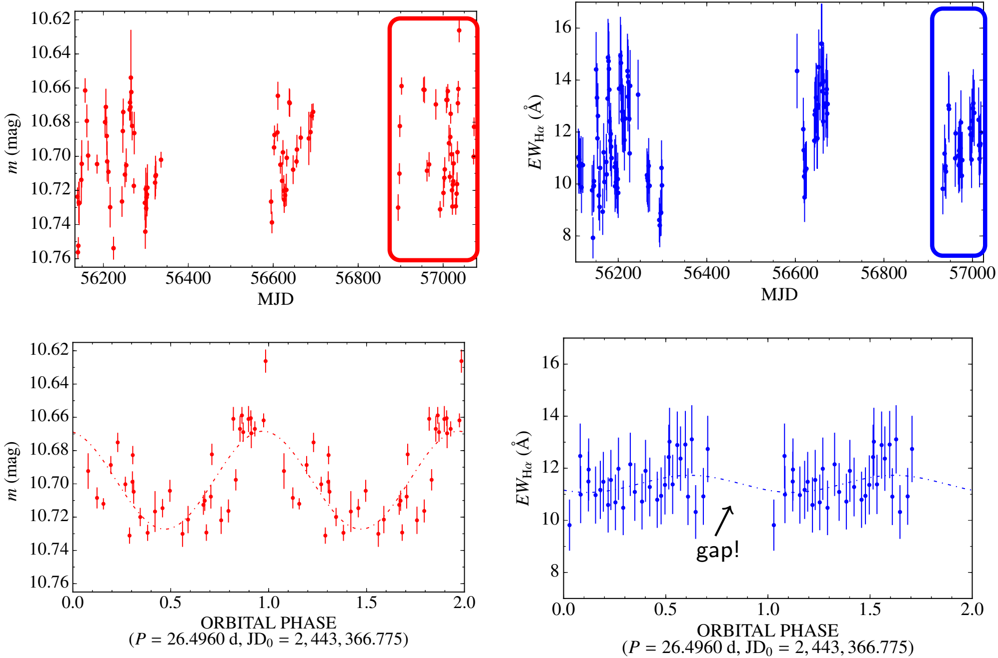

10.62
10.64
10.66
10.68
10.70
10.72
10.74
10.76
m (mag)
56200
56400
56600
56800
57000
MJD
16
14
12
10
8
$EW_{H\alpha}$ (Å)
56200
56400
56600
56800
57000
MJD
10.62
10.64
10.66
10.68
10.70
10.72
10.74
10.76
m (mag)
0.0
0.5
1.0
1.5
2.0
ORBITAL PHASE
(P = 26.4960 d, JD_0 = 2, 443, 366.775)
16
14
12
10
8
$EW_{H\alpha}$ (Å)
gap!
0.0
0.5
1.0
1.5
2.0
ORBITAL PHASE
(P = 26.4960 d, JD_0 = 2, 443, 366.775)

Results IV

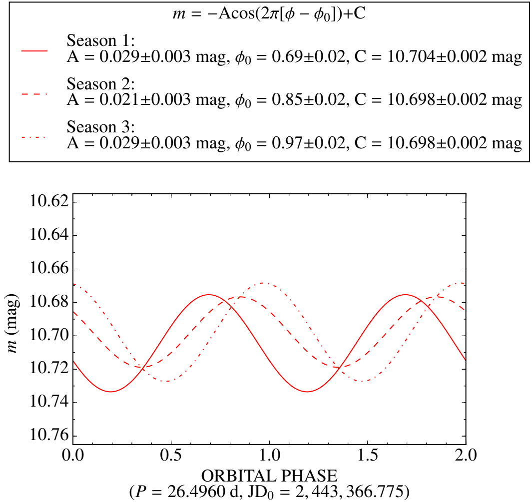
$m = -A\cos(2\pi[\phi - \phi_0])+C$
Season 1:
A = 0.029±0.003 mag, ϕ_0 = 0.69±0.02, C = 10.704±0.002 mag
Season 2:
A = 0.021±0.003 mag, ϕ_0 = 0.85±0.02, C = 10.698±0.002 mag
Season 3:
A = 0.029±0.003 mag, ϕ_0 = 0.97±0.02, C = 10.698±0.002 mag
m (mag)
ORBITAL PHASE
(P = 26.4960 d, JD_0 = 2, 443, 366.775)

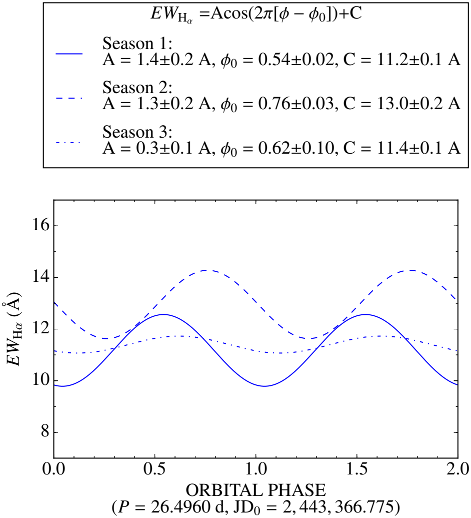
$EW_{H_\alpha} = A\cos(2\pi[\phi - \phi_0])+C$
Season 1:
A = 1.4±0.2 A, ϕ_0 = 0.54±0.02, C = 11.2±0.1 A
Season 2:
A = 1.3±0.2 A, ϕ_0 = 0.76±0.03, C = 13.0±0.2 A
Season 3:
A = 0.3±0.1 A, ϕ_0 = 0.62±0.10, C = 11.4±0.1 A
$EW_{H\alpha}$ (Å)
ORBITAL PHASE
(P = 26.4960 d, JD_0 = 2, 443, 366.775)

Results IV

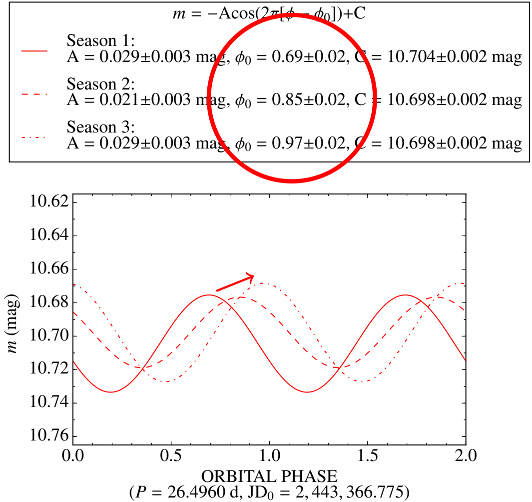
m = −Acos(2π[φ − φ₀])+C
Season 1:
A = 0.029±0.003 mag, φ₀ = 0.69±0.02, C = 10.704±0.002 mag
Season 2:
A = 0.021±0.003 mag, φ₀ = 0.85±0.02, C = 10.698±0.002 mag
Season 3:
A = 0.029±0.003 mag, φ₀ = 0.97±0.02, C = 10.698±0.002 mag
m (mag)
10.62
10.64
10.66
10.68
10.70
10.72
10.74
10.76
0.0
0.5
1.0
1.5
2.0
ORBITAL PHASE
(P = 26.4960 d, JD₀ = 2, 443, 366.775)

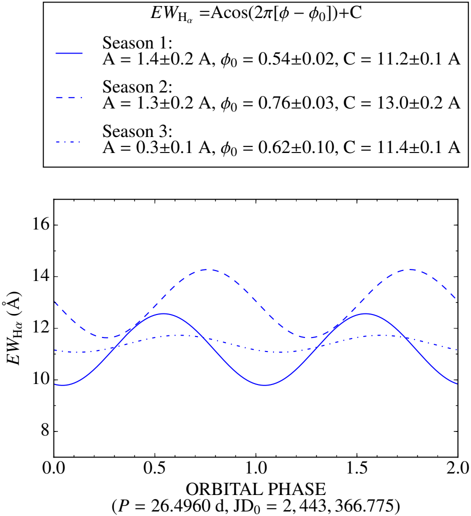
EW_Hα =Acos(2π[φ − φ₀])+C
Season 1:
A = 1.4±0.2 A, φ₀ = 0.54±0.02, C = 11.2±0.1 A
Season 2:
A = 1.3±0.2 A, φ₀ = 0.76±0.03, C = 13.0±0.2 A
Season 3:
A = 0.3±0.1 A, φ₀ = 0.62±0.10, C = 11.4±0.1 A
EW_Hα (Å)
16
14
12
10
8
0.0
0.5
1.0
1.5
2.0
ORBITAL PHASE
(P = 26.4960 d, JD₀ = 2, 443, 366.775)

Results IV

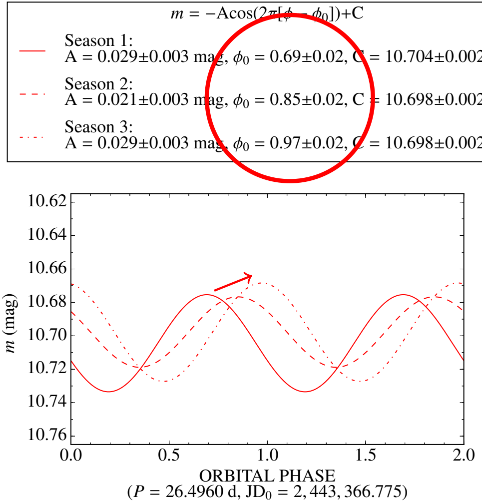
m = −Acos(2π[φ − φ0])+C
Season 1:
A = 0.029±0.003 mag, φ0 = 0.69±0.02, C = 10.704±0.002 mag
Season 2:
A = 0.021±0.003 mag, φ0 = 0.85±0.02, C = 10.698±0.002 mag
Season 3:
A = 0.029±0.003 mag, φ0 = 0.97±0.02, C = 10.698±0.002 mag
m (mag)
10.62
10.64
10.66
10.68
10.70
10.72
10.74
10.76
0.0
0.5
1.0
1.5
2.0
ORBITAL PHASE
(P = 26.4960 d, JD0 = 2, 443, 366.775)

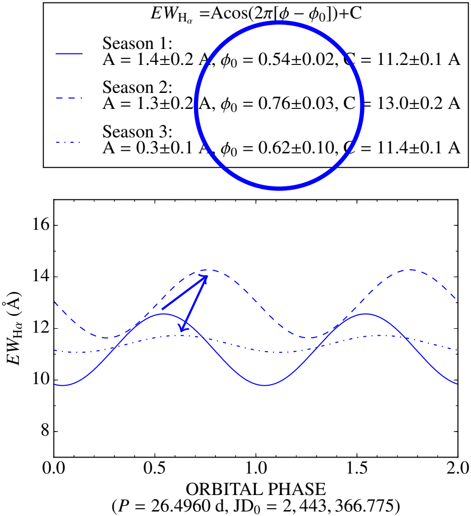
EWHα =Acos(2π[φ − φ0])+C
Season 1:
A = 1.4±0.2 A, φ0 = 0.54±0.02, C = 11.2±0.1 A
Season 2:
A = 1.3±0.2 A, φ0 = 0.76±0.03, C = 13.0±0.2 A
Season 3:
A = 0.3±0.1 A, φ0 = 0.62±0.10, C = 11.4±0.1 A
EWHα (Å)
16
14
12
10
8
0.0
0.5
1.0
1.5
2.0
ORBITAL PHASE
(P = 26.4960 d, JD0 = 2, 443, 366.775)

Results V

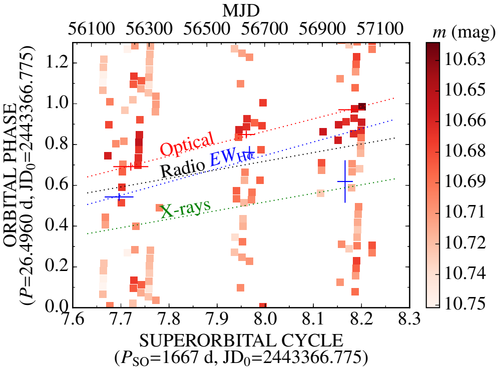

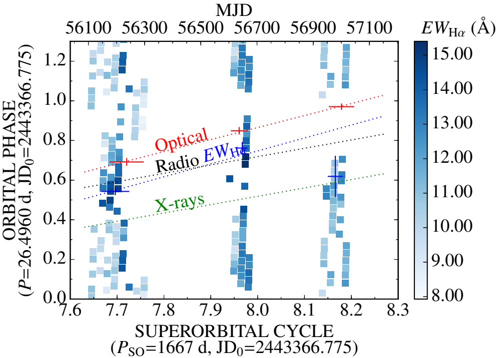

- The red and blue crosses correspond to the **phases of the maxima** of the sinusoidal fits to the orbital variability of the Optical and $EW_{\mathrm{H}\alpha}$, respectively.
- The color lines represent the **orbital phase drift** of the emission peaks caused by the **super-orbital variability** for the Optical, $EW_{\mathrm{H}\alpha}$, Radio, and X-rays.
- The Radio and X-ray drifts are taken from Fig. 3 of Chernyakova et al. (2012) using data of the previous superorbital cycle.

Outline

Discussion I

Orbital variability:

- The **circumstellar disk** is likely to be **perturbed** by tidal forces and the putative pulsar wind ram pressure. **After periastron passage** at $\phi_{\rm per} = 0.23$:

1. There is first a maximum in X-rays (tracer of **nonthermal emission**)
2. Followed by a maximum in $EW_{\mathrm{H}\alpha}$ (tracer of the **outer disk** conditions) and in Radio emission (produced mainly **outside the binary** system)
3. Finally a maximum in the Optical flux is observed (variability from **inner circumstellar disk**)

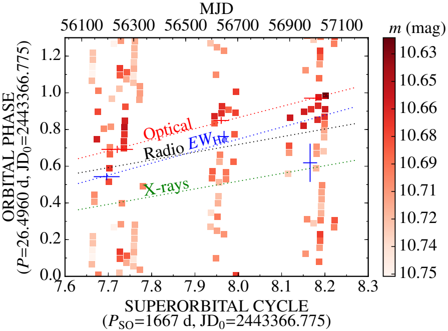

- Optical flux shows ~ 0.06 mag modulation (in 1st season), or $\sim 6\%$ in total flux. The Be disk represents the 35% of the flux (Casares et al. 2005). Variability is $\sim 16\%$ in disk flux
- $EW_{\mathrm{H}\alpha}$ shows $\sim 25\%$ variability (1st season): **external parts of the disk are more perturbed**
- There is a ~ 0.1 phase lag between the Optical and $EW_{\mathrm{H}\alpha}$: the **external parts are perturbed (and recover) before the internal parts**

Discussion II

Superorbital variability:

- $EW_{\mathrm{H}\alpha}$ superorbital variability is associated with **periodic changes on the Be star** (e.g., Zamanov et al. 1999)
- This secular evolution could be linked to the presence of a **moving one-armed spiral density wave in the disk** (Negueruela et al. 1998)
- We detect an orbital phase drift in the optical as that seen in Radio and X-rays.
- **Empirical coupling between the thermal (optical) and nonthermal (X-ray and radio) emission**

Future work:

- Continue the observations of LS I +61 303.
- Build a toy model (precessing disk or densit wave) to explain the thermal behaviour.